

CERTIFICATION

We certify that this thesis entitled "*Flow Calculations Through Gas Turbine Blade Passage*" was prepared by "*Rana Ali Hussien*" under our supervision at **Babylon University**, College of Engineering in partial fulfillment of the requirements for the degree of Master of Science in Mechanical Engineering.

Signature:

Name: Asst. Prof.

Dr.Arkan K. Al-Taie

(Supervisor)

Date: / / ٢٠٠٣

Signature:

Name: Asst. Prof.

Dr.Abdul Kareem A.Wahab

(Supervisor)

Date: / / ٢٠٠٣

حسابات الجريان بين ريش التوربين الغازي

أطروحة

مقدمة إلى كلية الهندسة في جامعة بابل كجزء من متطلبات نيل درجة

ماجستير علوم في الهندسة الميكانيكية

أعدت من قبل

رنا علي حسين بدير

تموز ٢٠٠٣

**Ministry of Higher Education and Scientific Research
Babylon University
College of Engineering
Department of Mechanical Engineering**

Flow Calculations Through Gas Turbine Blade Passage

A Thesis

**Submitted to the College of Engineering
of the University of Babylon in Partial
Fulfillment of the Requirements
for the Degree of the Master
of Science in Mechanical
Engineering**

By

RANA ALI H.BDIER

B.Sc. ٢٠٠٠

Supervisors

Dr.

Arkan K.Al-Taie

Dr.

Abdul Kareem A.Wahab

July ٢٠٠٣

Abstract

A developed procedure is presented for aerodynamic design of an axial flow through gas turbine stage. The mathematical model considered depends upon operating conditions of the turbine, property specifications of working fluid and geometric constraints as required input data. Power, efficiency, and the design parameters of the turbine stage are predicted for computed several steps of blade geometry redefinition and blade passage flow analysis by using a computer program developed for this purpose. The study of the distribution of Mach number, pressure, velocity and fluid density along the blade by using Euler equations by mapping the physical domain to a computational domain is performed by using time marching technique. The MacCormack method is used to solve unsteady, inviscid and two-dimensional flow using finite difference method. The inlet conditions used are $T_t = 1300 \text{ K}$, $P_t = 1 \text{ (atmosphere)}$. It is found that the optimum values of design parameters are: the swirl angle $\alpha_3 = 10 \text{ (deg.)}$, which gives turbine efficiency of 94% and total pressure (expansion) ratio of 0.37 . The number required of rotor blades and stator blades is found by using aerodynamic analysis. An accuracy of 3% in pressure ratio was seen when comparing the obtained results with the published data. The fourth order artificial viscosity terms have been used to achieve the stability and accuracy of flow computational techniques and stable is obtained after about the number of iteration 2000 .

Chapter one**INTRODUCTION****1.1 General**

Axial flow gas turbines are turbomachines that expand a continuously flowing fluid essentially in the axial direction. Development of the axial flow gas turbine was hindered by the need to obtain both a high flow rate and a compression ratio from a compressor to maintain the air requirement for the combustion process and the subsequent expansion of the hot gases. Axial flow turbine has very wide applications ranging from aircraft propulsion to industrial and marine plants. Gas turbines are used, as the power unit for the large jet aircraft propulsion, because they have a very high power to the weight ratio as compared to reciprocating I.C.Es. In the case of aircraft jet propulsion, to have enough jet thrust, high axial velocities are desirable. At most two rows of nozzles and blades are required to form the turbine unit. But, gas turbines, which are used in industrial or marine plants, require a larger number of stages. This is required to reduce the carryover loss, and to reduce the load on the blades to give the turbine a long working lifetime. The principle of energy extraction from the gas is represented gradually by reducing the high-pressure energy by converting it into kinetic energy then utilize this energy to push rotor blades. This is accomplished by passing the gas alternately through rows of fixed and moving blades. The kinetic energy of the gas is reduced in the moving blades, which are attached to the turbine hub and increased in the stationary blades attached to the casing. The density of the gas gradually decreases as the gas moves through the turbine, and to maintain a constant axial flow velocity, the blade height is increased towards the low pressure end. For compressible fluids there is

the well-known steam turbine with its relatively long history backed by many years of experience and the newer application of the gas turbine, which although no newer in concept, has only become of major importance in the last decade, because its successful use had to wait for the development of efficient compressors and of materials of high strength at elevated temperatures.

Practically any information relating to the behavior of steam turbine blading is applicable to gas turbine blading and vice versa. The difference in analysis lies largely in the fact that in most applications the gas turbine must be made to work with the utmost efficiency because of the nature of its associated thermodynamic cycle. Whereas, although such a criterion is desirable for steam turbines, their working conditions are such that economy in manufacturing cost and requirements of long life have taken precedence over fractional increases of efficiency. Furthermore, the steam turbine was developed to give a high performance before the science of aerodynamics had reached its present state and thus many of data available for design are in a semiempirical state, often in an uncorrelated form when looked at from the aerodynamic viewpoint .

The history of turbines dates back several hundred years, starting with windmills, steam turbines, and water turbines eventually leading to gas turbines. The gas turbine is a relative newcomer. The flow in turbines, unlike that in compressors, is much better behaved, in view of the favorable pressure gradients that exist. Therefore, they are easier to design. Large pressure drop can be achieved per stage without the danger of separating the flow, therefore, fewer stages are required in operating turbines as compared to compressors to achieve the same change in pressure. Therefore, much higher efficiencies can be achieved in turbine stage.

The turbine has difference problems that are not present in compressors, the presence of high-temperature gases introduces higher stresses and decreases lifetime-also, the presence of particles in combustion products results in erosion of blading. [۱]

The mass flow of a gas turbine engine, which is limited by the maximum permissible Mach number entering the compressor, is generally large enough to require an axial turbine. The axial turbine is essentially the reverse of the axial compressor except for one essential difference: The turbine flow operates under a favorable pressure gradient. This permits greater angular changes, greater pressure changes, greater energy changes, and higher efficiency. However, there is more blade stress involved because of higher work and temperatures. A modern turbine is merely an extension of these basic concepts. Considerable care is taken to establish a directed flow of fluid with high velocity by means of stator blades, and then similar care is used in designing the blades on the rotating wheel. The appreciation comes when one witnesses a static test of the stator blades which direct a gas stream to the rotor of a modern aircraft gas turbine. In the gas turbine, the high-pressure, high-temperature gas from the combustion chamber flows in an annular space to the stationary blades (called stators, vanes, or nozzles) and is directed tangentially against the rotating blade row (called rotor blades).

In many axial turbines, the hub and tip diameters vary little through the machine, and the hub-tip ratio approaches unity. There can be no large radial components of velocity between the annular walls in such machines, there is a little variation in the static pressure from the root to the tip and the flow conditions are little different at each radius [۲,۳].

As mentioned earlier, the simple implicit techniques are difficult to apply to nonlinear problems and require large computer time. Even the explicit techniques suffer from similar problems when dealing with nonlinear, two- and three-dimensional problems. Freziger (1981) provides a list of problems associated with the simple explicit and implicit techniques and the reasons for resorting to the splitting technique. The MacCormack method is an explicit finite difference technique, which is second-order-accurate in both space and time.

The algebraic expression is used to transform the body shape in the physical domain into rectangular shape in the computational domain in the algebraic grid generation technique. In the algebraic grid generation scheme, known functions are used to map the curvilinear coordinate system in the physical space to a convenient (usually rectangular) system in the computational domain. Eiseman (1982) and Smith (1983) provide details of the basic technique for two-dimensional and three-dimensional algebraic grid generation methods. This technique is based on the use of interpolation functions.

The turbine considered in the present work is a single stage of axial flow gas turbine and the explicit method is used to calculate the fluid properties on the suction and pressure surfaces of the blade and the Euler equations governed the motion of an inviscid, non heat-conducting fluid flow regimes.

1.2 Work Objectives

The aim of the present work is to achieve the following objectives

1. Design a single-stage axial flow gas turbine with high work output.
2. Study the flow conditions in turbine blade passages using time marching method.

۳. Construct a computer program to implement the computational steps in design procedure with the capability of studying the effects of design variables (inlet absolute flow angle, blade speed ratio, inlet and outlet angles of blades) on a turbine performance namely efficiency and power .

۱.۳ Layout of the thesis

The thesis falls into five chapters .Chapter one is an introduction , Chapter two is concerned with a brief literature review . Chapter three is divided into four sections ; section one presents the aerodynamic design , section two presents the grid generation ,section three presents the analytical solution and section four presents the computer programs . Chapter four presents the results and their discussion and chapter five presents the conclusions drawn from this work with suggestions for further work .

Chapter Two

٦

LITERATURE REVIEW

Pratt and Whitney, ١٩٨٢,[٤], Present a fast explicit numerical scheme for solving the unsteady Euler flow equations to obtain steady solutions. The scheme is constructed by combining the multiple-grid technique with a new second –order accurate finite volume integration method. Special formulas, consistent with local wave propagation are utilized to determine corrections of flow properties at each grid point. These formulas are found to provide useful insights into the solution procedure. Calculated results for both internal and external flow problems are given to demonstrate the accuracy and the computational efficiency of this scheme.

Denton , ١٩٨٣,[٥] Outlines the time-marching solutions of the Euler equations which are very widely used for calculation of the flow through turbomachinery blade rows . All methods suffer from the disadvantages of shock smearing, lack of entropy conservation and comparatively long run times. A new method is described which reduces all these problems. The method is based on the author opposed difference scheme but this is applied to a new grid consisting of quadrilateral elements which do not overlap and have nodes only at their corners .The use of a non-overlapping grid reduces finite differencing errors and gives a complete freedom to vary the size of the elements. Both these factors help to improve entropy conservation. Considerable savings in run time (by a

factor of about 3) are obtained by using a simple multigrid method whereby the solution is advanced simultaneously on a coarse and on a fine grid. The resulting method is simpler, faster, and more accurate than its predecessor.

Eidelman and Shreeve, 1984,[6], Discuss the Godunov method and a new second-order accurate extension of the method which are used for the solution of two-dimensional Euler equations. Their performances in the subsonic, transonic and supersonic flow regimes are first tested on the problem of flow in a channel with a circular bump. The methods are then applied to calculate the transonic flow through a supercritical compressor cascade designed by Sanz. For this case, the solution with the second-order extension of the Godunov method gives a very good agreement.

Mao, 1984,[7], Presents a streamline curvature method for calculating surface flow in turbines. The streamline curvature is a simple method in which a domain of calculation can be changed into an orderly rectangle without making coordinate transformations. Calculation results obtained on subsonic and transonic turbine cascades have been compared with those of the experiment. A good agreement has been found. When calculating blade-to-blade flow velocity at subsonic speed, a function approximation technique can be used in lieu of iteration method in order to reduce calculation time.

Clarke, 1986,[8], Analyzes a finite volume formulation for the Euler equations by using Cartesian grids complex two-dimensional configurations. The formulation extends methods developed for the potential equation to the Euler equations. Results using this approach for

single –element airfoils are shown to be competitive with, and as accurate as, other methods that employ mapping grids. Further, it is demonstrated that this method provides a simple and an accurate procedure for solving the flow problems involving multielement airfoils.

Jameson , 1986,[9], Describes a multigrid method for implicit schemes of the approximate factorization type. The application of the method coupled with an alternating direction implicit scheme to the solution of the Euler equations for transonic flow over an airfoil has resulted in very rapid convergence. The number of time steps required to reach a steady state is reduced by an order of magnitude by the introduction of multiple grids. The multigrid method can dramatically accelerate the convergence of transonic potential flow calculations, although the governing equations are of mixed elliptic and hyperbolic type. In its published form his distributed correction scheme includes an artificial dissipation term that restricts the results to first-order accuracy. A new multigrid method which is a second –order –accurate in space was developed for the multistage explicit time stepping scheme.

Moon, 1986,[10], Presents a new efficient procedure for the numerical solution of Navier-Stokes equation, using line Gauss-Seidel and Newton iterative methods which are recently presented by McCormack. The numerical procedure was applied to the compressible viscous flow of a two-dimensional flow within a transonic converging-diverging nozzle. Although the present method showed a very high numerical efficiency, the fact that the grid size might severely affect convergence was questionable. It was suggested that the number of iterations would vary directly with the number of grid points. The effect

of grid size on convergence was tested by refining the grid size by factors of two and four for the same transonic problem presented by McCormack.

Wornom and Hafez, 1986,[11], Present a new approach to a characteristic modeling scheme that does not require the governing equations to be written in characteristic variables or the flux terms to be split into positive and negative parts. The method is based on the observation, that for certain finite volume schemes, the upwind influence can be accounted for through the conditions applied at the boundaries of individual cells instead of flux differencing. The method is developed and applied to the one-dimensional nozzle flow equations for subsonic, transonic, and supersonic flows and is then extended to two dimensions using an approximate factorization. For the problem of a shock wave reflecting from a flat plate, the present solution algorithm reduces the computational work per time step by 40% of that required by standard, central difference, implicit, calculations.

Pulliam, 1986,[12], Analyzes various artificial models that are central difference algorithms for the Euler equations for their effect on accuracy, stability and convergence rates. In particular, linear and nonlinear models are investigated by using an implicit approximate factorization code for transonic airfoils. It is shown that accurate, error free solutions with sharp shocks can be obtained using a central difference algorithm coupled with an appropriate nonlinear artificial dissipation model.

Belk, 1987,[13], Discusses an explicit upwind second-order accurate predictor-corrector finite volume scheme used to solve the unsteady three-dimensional Euler equations on a dynamic body-following grid. A method for calculating fluxes at cell faces that eliminates the upstream propagation of information in supersonic regions is presented. The unsteady Euler equations are solved for the prescribed motion of a body, and time-accurate aerodynamic forces on the body are compared with forces obtained by a quasisteady approximation.

Lavante, 1987,[14], Presents the development of a numerical method for solving the two-dimensional Euler equations for steady-state solutions by using flux vector splitting. The equations are expressed in curvilinear coordinates and the finite volume approach is used. The energy equation is omitted since only steady-state solutions are required. A simplified implicit operator is employed to reduce the computational effort of the present method. Convergence characteristics are compared with predictions obtained by other authors.

Venkatakrishnan, 1988,[15], Uses a finite volume scheme to spatially discretize the integral form of the Euler equations for a moving domain. The first method uses dissipative terms constructed according to the theory of total variation diminishing (or TVD) schemes. The TVD scheme is presented in a semidiscrete form for a scalar conservation law and then is formally extended to a system of conservation laws. The resulting system of ordinary differential equations are integrated in time by a multistage scheme. A new class of multistage schemes that preserve the TVD property is used. The technique of residual averaging, which permits the use of larger time steps is extended to unsteady problems in a

form that preserves time accuracy. The second method utilizes dissipative terms constructed from second and fourth differences in the dependent variables. Nonreflecting boundary conditions are used in the far field, allowing the use of a moving mesh.

Gerolymos, 1988,[16], Has developed an algorithm for numerically integrating the Euler equations in blade-to blade surface formulation. The method simulates all the interblade channels of an annular cascade. The equations are discretize in a grid that moves in order to follow the vibration of the blades. The equations are integrated by using the explicit MacCormack scheme in finite- difference formulation. A number of numerical results show the aptitude of the method to simulate both started and unstarted supersonic flow in vibrating cascades.

Kwon, 1988,[17], Presents a robust, time-marching Navier-Stokes solution procedure based on the explicit hopscotch method for the solution of steady, two-dimensional, transonic turbine cascade flows. The method is applied to the strong conservation form of the unsteady Navier-Stokes equations written in arbitrary curvilinear coordinates. Cascade flow solutions are obtained on an orthogonal, body-conforming grid. A reliable Navier-Stokes solution procedure has been presented for the prediction of two-dimensional, compressible, transonic flows in turbomachinery cascades. The solution procedure developed by Kwon and Delaney for transonic nozzle flow was generalized to arbitrary curvilinear coordinates for application to a grid system. The method is computationally explicit and has a substantial computational speed advantage for steady flow analyses over other explicit schemes not utilizing multigrid acceleration. An orthogonal, body-conforming grid has been used for solution of the turbine cascade flows.

Oguz , ۱۹۹۵,[۱۸], Presents a construction of a very fast, loosely coupled, quasi-three-dimensional design system for the preliminary prediction of the turbomachinery blade shapes. It is obtained by coupling a duct-flow solver and a blade-to-blade solver. The duct-flow solver is used for calculating the upstream and downstream radial evolutions of the flow variables. The blade-to-blade solver is a two-dimensional transonic Euler solver which uses intrinsic streamline grid, a cell-centered finite volume scheme and Newton-Raphson linearization technique. The unknowns are reduced to two, density and grid node displacement, at each grid node and this creates the speed of the blade-to-blade solver, thus the design system. After the radial distributions of the flow variables are determined by the duct-flow solver, the blade-to-blade solver is run at each radial station, firstly in analysis mode. For the rotor blades, the loading which results from this calculation is compared with the desired one and accordingly the blade shape is modified by changing the lift on the blade and running the blade-to-blade solver, now in design mode. Similar design procedure is applied for the design of stator blades and the turning angle is used as the design target instead of the loading. A sample design is accomplished for a rotor and a stator blade. The blade-to-blade solver is applied to two analytical test cases for the verification of the analysis and design capability and an experimental rotor test case for the verification of the modification of the code for the rotating frame of reference. Being an inviscid solver and the lack of possibility of the three-dimensional effects due to the loose coupling of the duct-flow solver and the blade-to-blade solver is the main drawbacks of the method

Montgomery and Verdon, ۱۹۹۶,[۱۹], Present an analysis of three-dimensional, linearized, Euler developed to provide an efficient unsteady

aerodynamic analysis that can be used to predict the aeroelastic and aeroacoustic response characteristics of axial-flow turbomachinery blading. The field equations and boundary conditions needed to describe nonlinear and linearized inviscid unsteady flows through a blade row operating within a cylindrical annular duct. In addition, a numerical model for linearized inviscid unsteady flow, which is based upon an existing nonlinear, implicit, wave-split, finite volume analysis, is described. These aerodynamic and numerical models have been implemented into an unsteady flow code, called LINFLUX. A preliminary version of the LINFLUX code is applied to select, benchmark three-dimensional, subsonic, unsteady flows, to illustrate its current capabilities and to uncover existing problems and deficiencies. The numerical results indicate that good progress has been made toward developing a reliable and useful three-dimensional prediction capability. However, some problems, associated with the implementation of an unsteady displacement field and numerical errors near solid boundaries, still exist. Also, accurate far-field conditions must be incorporated into the LINFLUX analysis, so that this analysis can be applied to unsteady flows driven by external aerodynamic excitations.

Ning, ۱۹۹۸,[۲۰], Presents a quasi-three-dimensional time-linearized Euler method developed to compute unsteady flows around oscillating blades. In the baseline method, unsteady flow is decomposed into a steady flow plus a linear harmonically varying unsteady flow. Both the steady flow equations and the unsteady perturbation equations are solved by using a pseudo-time-marching method. Based upon this method, a novel nonlinear harmonic Euler method has been developed. Due to the nonlinearity of the aerodynamic governing equations, time averaging generates extra (unsteady stress) terms. These nonlinear effects

are included by a strongly coupled approach between the perturbation equations and the time-averaged equations. Numerical results demonstrate that nonlinear effects are very effectively modeled by the nonlinear harmonic method.

Demeulenaere, 1998,[21], Outlines an iterative procedure for three-dimensional blade design, in which the three-dimensional blade shape is modified by using a physical algorithm, based on the transpiration model. The transpiration flux is computed by means of a modified Euler solver, in which the target pressure distribution is imposed along the blade surfaces. Only a small number of modifications is needed to obtain the final geometry. A three-dimensional analysis code was successfully transformed into a design code, by changing the boundary conditions on the blade walls, and by means of a geometry modification algorithm. The method shows a rapid convergence to the blade geometry corresponding to the target pressure distribution, for subsonic and transonic design. The solver is able to treat highly three-dimensional flows and geometries, and the effects of a blade lean are taken into account, which is considered as an advantage, when compared to two-dimensional design methods. An important advantage of the method is the possibility of using the same code for the design and analysis of a blade.

Amano, 2000,[22], Presents a time-marching algorithm that have been mostly used in gas turbine cascade flow analyses. A new efficient implicit scheme based on the second-order time and spatial difference algorithm for solving steady flow by using time-marching Navier-Stokes equations, was developed for predicting turbine cascade flows. The

difference scheme comprises an explicit part in the intermediate time-step and an implicit part in the local time-step. The viscous flux vectors are decomposed to simplify the flow calculation in the explicit step. The time difference terms are expressed in terms of the viscous dependent terms that appear in the diffusion terms in the form by adding eigenvalues of viscous flux matrices into the time derivation term. This method has been used to calculate the flow around cascades. The computed results were compared with experimental data as well as with other published computations. The comparisons for both surface pressures showed a good agreement with experiments.

Summary

There are many techniques to deal with the numerical analysis of the Euler equations such as , the Godunov method ,streamline curvature method for calculating surface flow in turbines , finite volume method , multigrid for implicit schemes .

In the present work , unsteady , compressible , two dimensional , adiabatic flow through turbine cascade will be modeled by using Euler equations and the explicit time-dependent solution by using McCormack predictor corrector finite difference technique to solve the given system of differential equations .

Chapter Three

THEORY OF BLADE DESIGN

3.1 Aerodynamic design

3.1.1 INTRODUCTION:

A single stage gas turbine is considered. It consists of a nozzle followed by rotor as shown in Figure. (3.1), [23].

The following assumptions are made:

1. The turbine is an axial type.
2. The flow is frictionless.
3. Adiabatic expansion.

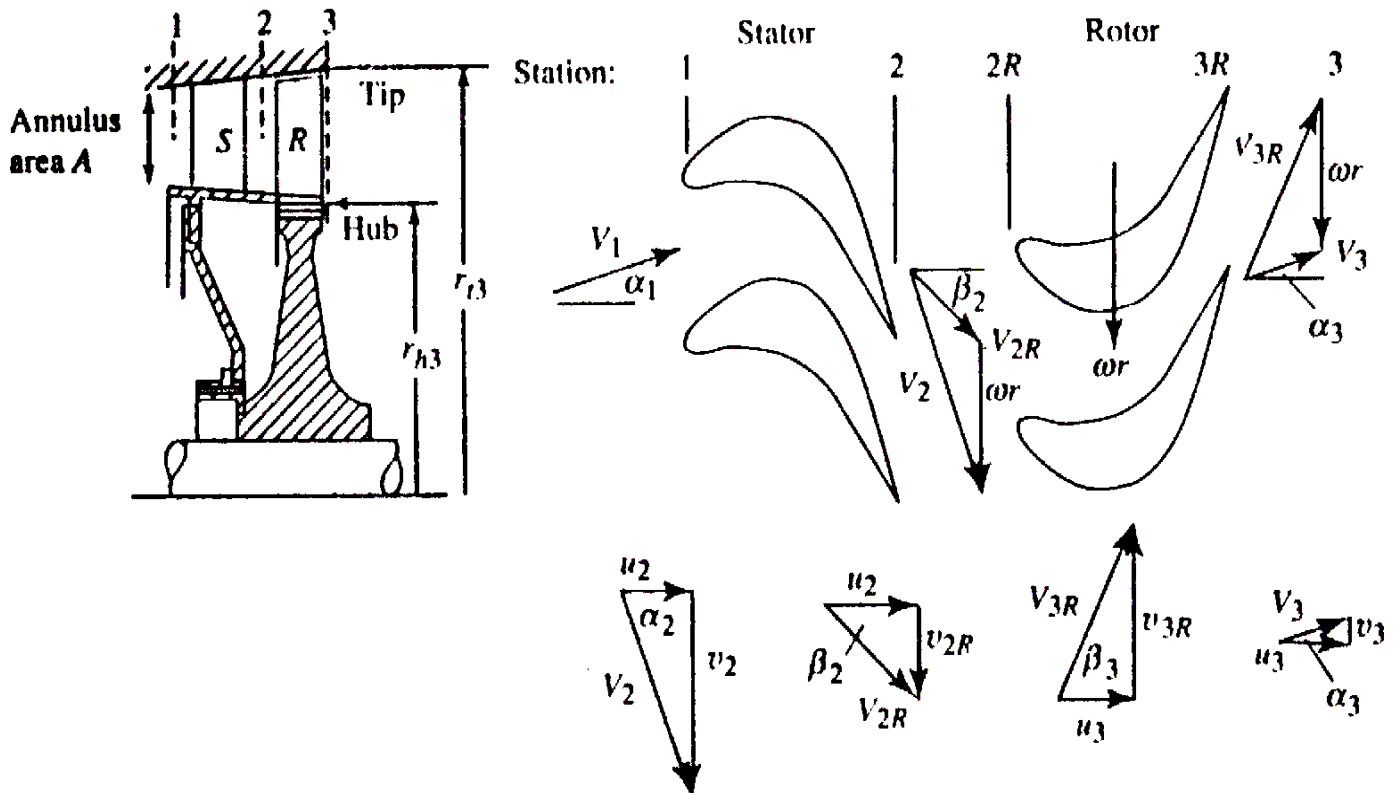


Figure (3.1)
Axial flow turbine stage [23]

Dimensional stage, the flow velocity, blade speed and pressure are assumed constant along the blade length. Also, turbine cooling is neglected.

The mathematical model developed is based upon the following equations as shown in fig (r. 1):

Inlet static temperature is calculated as follows

$$T_1 = \frac{T_{t1}}{1 + [(\gamma - 1)/2] * M_1^2} \dots\dots\dots (1)$$

The absolute velocity

$$V_1 = \sqrt{\frac{2CP T_{t1}}{1 + 2/[(\gamma - 1)M_1^2]}} \dots\dots\dots (2)$$

From velocity triangles

$$U_1 = V_1 \cos \alpha_1 \dots\dots\dots (3)$$

For isothermal flow

$$T_{t2} = T_{t1} \dots\dots\dots (4)$$

The static temperature exit from stator

$$T_2 = \frac{T_{t2}}{1 + [(\gamma - 1)/2] * M_2^2} \dots\dots\dots (5)$$

The absolute velocity exit from stator

$$V_2 = \sqrt{\frac{2CP T_{t2}}{1 + 2/[(\gamma - 1)M_2^2]}} \dots\dots\dots (6)$$

The stage loading coefficient which is the ratio of stage work to rotor speed square

$$\Psi = \frac{cp(T_{t1} - T_{t3})}{(\omega r)^2} \dots\dots\dots$$

(V)

The velocity ratio = rotor speed / tangential velocity

$$VR = \frac{1}{\sqrt{2\Psi}} \dots\dots\dots(\wedge)$$

The exit absolute velocity angle

$$\alpha_2 = \sin^{-1} \frac{\psi \frac{\omega r}{V_2} - \frac{u_3}{u_2} \tan \alpha_3 \sqrt{1 + \left(\frac{u_3}{u_2} \tan \alpha_3\right)^2 - \left(\psi \frac{\omega r}{V_2}\right)^2}}{1 + \left(\frac{u_3}{u_2} \tan \alpha_3\right)^2} \dots\dots(\text{q})$$

The axial velocity exits from stator

$$u_2 = V_2 \cos \alpha_2 \dots\dots\dots(10)$$

The tangential velocity inlet to the rotor

$$v_2 = V_2 \sin \alpha_2 \dots\dots\dots(11)$$

The absolute velocity at exit

$$V_3 = \frac{u_3 \cos \alpha_2}{u_2 \cos \alpha_3} V_2 \dots\dots\dots(12)$$

The axial velocity exit from rotor

$$u_3 = V_3 \cos \alpha_3 \dots\dots\dots(13)$$

The tangential velocity exit from rotor

$$v_3 = V_3 \sin \alpha_3 \dots\dots\dots(14)$$

The degree of reaction is the ratio of enthalpy drop in the rotor to the enthalpy drop in the stage

$$R_t = 1 - \frac{1}{2\psi} \left(\frac{V_2}{\omega r} \right)^2 \left[1 - \left(\frac{u_3 \cos \alpha_2}{u_2 \cos \alpha_3} \right)^2 \right] \quad \dots\dots\dots (15)$$

The static temperature exit from rotor

$$T_3 = T_2 - R_t (T_{t1} - T_{t3}) \quad \dots\dots\dots (16)$$

Mach number at exit

$$M_3 = M_2 \frac{V_3}{V_2} \sqrt{\frac{T_2}{T_3}} \quad \dots\dots\dots (17)$$

Mach number inlet to the rotor

$$M_{2R} = M_2 \sqrt{\cos^2 \alpha_2 + \left(\sin \alpha_2 - \frac{\omega^* r}{V_2} \right)^2} \quad \dots\dots\dots (18)$$

Mach number exit from the rotor

$$M_{3R} = M_3 \sqrt{\cos^2 \alpha_3 + \left(\sin \alpha_3 - \frac{\omega r}{V_3} \right)^2} \quad \dots\dots\dots (19)$$

Total temperature exit from rotor

$$T_{t3R} = T_{t3} + \frac{V_3^2}{2c_p} \left[\cos^2 \alpha_3 + \left(\sin \alpha_3 + \frac{\omega r}{V_3} \right)^2 - 1 \right] \quad \dots\dots\dots (20)$$

From adiabatic

$$T_{t2R} = T_{t3R} \quad \dots\dots\dots (21)$$

The static pressure at inlet

$$P_1 = P_{t1} \left(\frac{T_1}{T_{t1}} \right)^{\gamma/(\gamma-1)} \quad \dots\dots\dots (22)$$

The stage temperature ratio is

$$\tau_s = \frac{T_{t3}}{T_{t1}} \quad \dots\dots\dots (۲۳)$$

The inlet relative velocity angle

$$\beta_2 = \tan^{-1} \frac{v_2 - \omega r}{u_2} \quad \dots\dots\dots (۲۴)$$

The exit relative velocity angle

$$\beta_r = \tan^{-1} \frac{v_r - \omega r}{u_r} \quad \dots\dots\dots (۲۵)$$

The total pressure exit from the stator

$$P_{t2} = \frac{P_{t1}}{1 + \phi_{\text{stator}} \left[1 - (T_2/T_{t2})^{\gamma/(\gamma-1)} \right]}$$

The static pressure exit from the stator

$$P_2 = P_{t2} \left(\frac{T_2}{T_{t2}} \right)^{\gamma/(\gamma-1)}$$

The total pressure inlet to the rotor

$$P_{t2R} = P_2 \left(\frac{T_{t2R}}{T_2} \right)^{\gamma/(\gamma-1)}$$

The total pressure exit from rotor

$$P_{t3R} = \frac{P_{t2R}}{1 + \phi_{\text{rotor}} \left[1 - (T_3/T_{t3R})^{\gamma/(\gamma-1)} \right]}$$

..... The static pressure at exit

$$P_3 = P_{t3R} \left(\frac{T_3}{T_{t3R}} \right)^{\gamma/(\gamma-1)}$$

The total pressure at exit

$$P_{t3} = P_3 \left(\frac{T_{t3}}{T_3} \right)^{\gamma/(\gamma-1)}$$

.....(30)

.....(31)

The stage pressure ratio is

$$\pi_s = \frac{P_{t3}}{P_{t1}}$$

.....(32)
The adiabatic efficiency is

$$\eta_t = \frac{1 - \tau_s}{1 - \pi_s^{(\gamma-1)/\gamma}}$$

.....(33)

3.1.2 Flow Path Dimensions

The annulus area at any station of a turbine stage is based on the flow properties (T_t , P_t , Mach number, and flow angle) at the mean radius and the total mass flow rate. Equation (34) is the easiest equation to be used to calculate the flow area at any station i is as follows [33]: -

$$A = \frac{m^o \sqrt{T_{ti}}}{P_{ti}(\cos \alpha_i) \text{MEP}(\text{Mi})} \quad \text{..... (34)}$$

The airfoil angles of both the rotor and the stator blades can be calculated from the flow angles, given the incidence angle and solidity for each and to obtain the exit airfoil angle, the following equation can be used as shown in fig (3.2):

The blade angle

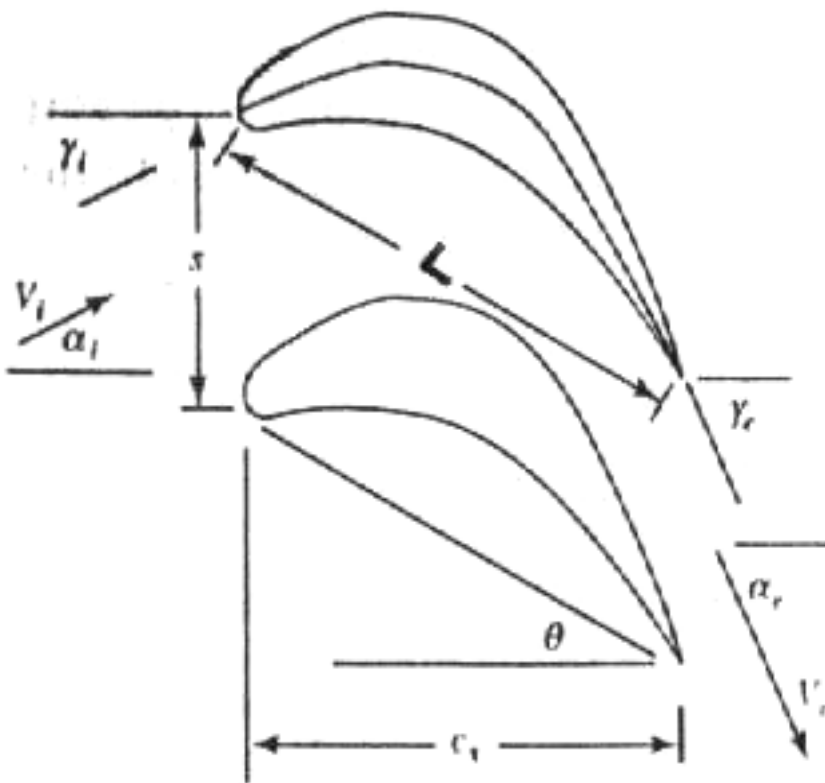
$$\gamma_{2i} = \frac{\gamma_{1i} + 8\sqrt{\sigma_i} \alpha_{2i}}{8\sqrt{\sigma_i} - 1} \dots\dots\dots (35)$$

The stagger angle

$$\theta_i = \frac{\gamma_{2i} - \gamma_{1i}}{2} \dots\dots\dots (36)$$

Where :-

$$\sigma_i = \frac{(c_x/s)_i}{\cos\theta_i} \dots\dots\dots (37)$$



- $\alpha_i - \gamma_i =$ incidence angle
- $\alpha_i + \alpha_e =$ turning angle
- $\gamma_e - \alpha_e = \delta_e =$ exit deviation
- $\gamma_i + \gamma_e =$ blade chamber
- $\sigma = c_x/s =$ solidity
- $\theta =$ stagger angle
- $c_x =$ axial chord

Fig (۳.۲) Blade angles

۳.۲ GRID GENERATION

Grid generation technique can be roughly classified into three categories[۲۴]:

۱. algebraic methods
۲. conformal mappings based on complex variables
۳. partial differential methods

Algebraic and differential equation techniques show the most promise for continued development when used in conjunction with finite difference methods.

Because the governing equations in fluid dynamics contain partial differentials and are too difficult in most cases to solve analytically, these partials are generally replaced by the finite difference terms. This procedure discretize the field into a finite number of states. These states, when plotted from a grid, or mesh of points or field points, can be obtained the solution. The numerical method generally used in CFD can be classified as finite difference, finite element, and finite volume.

The generation of a grid, with uniform spacing is a simple exercise within a rectangular physical domain. Grid points may be specified as coincident with the boundaries of the physical domain, thus making specification of boundary conditions considerably less complex.

Unfortunately, the majority of the physical domains of interest are nonrectangular.

Therefore, imposing a rectangular computational domain on such a physical domain will require some sort of interpolation for the implementation of the boundary conditions. Since the boundary conditions have a dominant influence on the solution of the equation, such an interpolation causes inaccuracies at the place of greatest sensitivity.

To overcome these difficulties, a transformation from physical space to computational space is introduced. This transformation is accomplished by specifying

a generalized coordinate system, which will map the nonrectangular grid system, the physical space to a rectangular uniform grid spacing in the computational space.

३.२.१ GRID GENERATION TECHNIQUES

The problem of grid generation is that of determining the mapping which takes the grid points from the physical domain to the computational domain. Several requirements must be placed on such mapping. Therefore a grid system with the following features is desired[२०]:

१. A mapping which guarantees one -to-one correspondence ensuring grid lines of the same family do not cross each other.
२. Smoothness of the grid distribution
३. Orthogonality or near orthogonality of the grid lines.
४. Options for grid clustering.

३.२.२ Algebraic Mesh Generation

The simplest grid generation technique is the algebraic method. The derivatives of the boundary in the physical plane provide even more flexibility in the mapping. For instance, orthogonality at the boundary can be forced in the physical plane. In most problems, the boundaries are not analytic function but are simply prescribed as a set of data points. In this case, the boundary must be approximated by a curve fitting procedure to employ algebraic mappings [२०,२१].

३.२.३ Assessment of Algebraic Grid Generator

The major advantages of algebraic methods (as compared to differential methods) are:

१. The speed , simplicity and flexibility with which a grid can be generated.
२. Algebraic procedures have low computational cost and explicit control of grid point distribution.

3. Matrix may be evaluated analytically, thus avoiding numerical approximation.
4. The ability to cluster grid points in different regions can be easily implemented.

The major disadvantages of algebraic methods are:

1. The grids are less smooth than those generated by the solution of PDEs.
2. Discontinuities at a boundary may propagate into the interior region, which could lead to errors due to the sudden changes in the metrics.

3.2.4 Generalized Coordinate Transformation

The equations of motion are transformed from the physical space (x,y) to computational space(ξ,η) as shown in figures (3.3) and (3.4), [34]:

$$\xi = \xi(x, y) \quad \dots\dots\dots (3.4a)$$

$$\eta = \eta(x, y) \quad \dots\dots\dots (3.4b)$$

The chain rule of partial differentiation provides the following expressions for the Cartesian derivatives:

$$\frac{\partial}{\partial x} = \frac{\partial}{\partial \xi} \frac{\partial \xi}{\partial x} + \frac{\partial}{\partial \eta} \frac{\partial \eta}{\partial x} \quad \dots\dots\dots (3.4a)$$

$$\frac{\partial}{\partial y} = \frac{\partial}{\partial \xi} \frac{\partial \xi}{\partial y} + \frac{\partial}{\partial \eta} \frac{\partial \eta}{\partial y} \quad \dots\dots\dots (3.4b)$$

Let, $\frac{\partial \xi}{\partial x} = \xi_x$ $\frac{\partial \xi}{\partial y} = \xi_y$

$$\frac{\partial \eta}{\partial x} = \eta_x \quad \frac{\partial \eta}{\partial y} = \eta_y$$

Equation (3.4) may be written in matrix forms as:

$$\begin{bmatrix} \frac{\partial}{\partial x} \\ \frac{\partial}{\partial y} \end{bmatrix} = \begin{bmatrix} \xi_x & \eta_x \\ \xi_y & \eta_y \end{bmatrix} \begin{bmatrix} \frac{\partial}{\partial \xi} \\ \frac{\partial}{\partial \eta} \end{bmatrix} \quad \dots\dots\dots (3.5)$$

The inverse transformation of equations (۳.۸) are defined as:

$$X = X(\xi, \eta) \dots\dots\dots (۳.۹a)$$

$$Y = Y(\xi, \eta) \dots\dots\dots (۳.۹b)$$

$$dx = x_{\xi} d\xi + x_{\eta} d\eta \dots\dots\dots (۳.۱۰a)$$

$$dy = y_{\xi} d\xi + y_{\eta} d\eta \dots\dots\dots (۳.۱۰b)$$

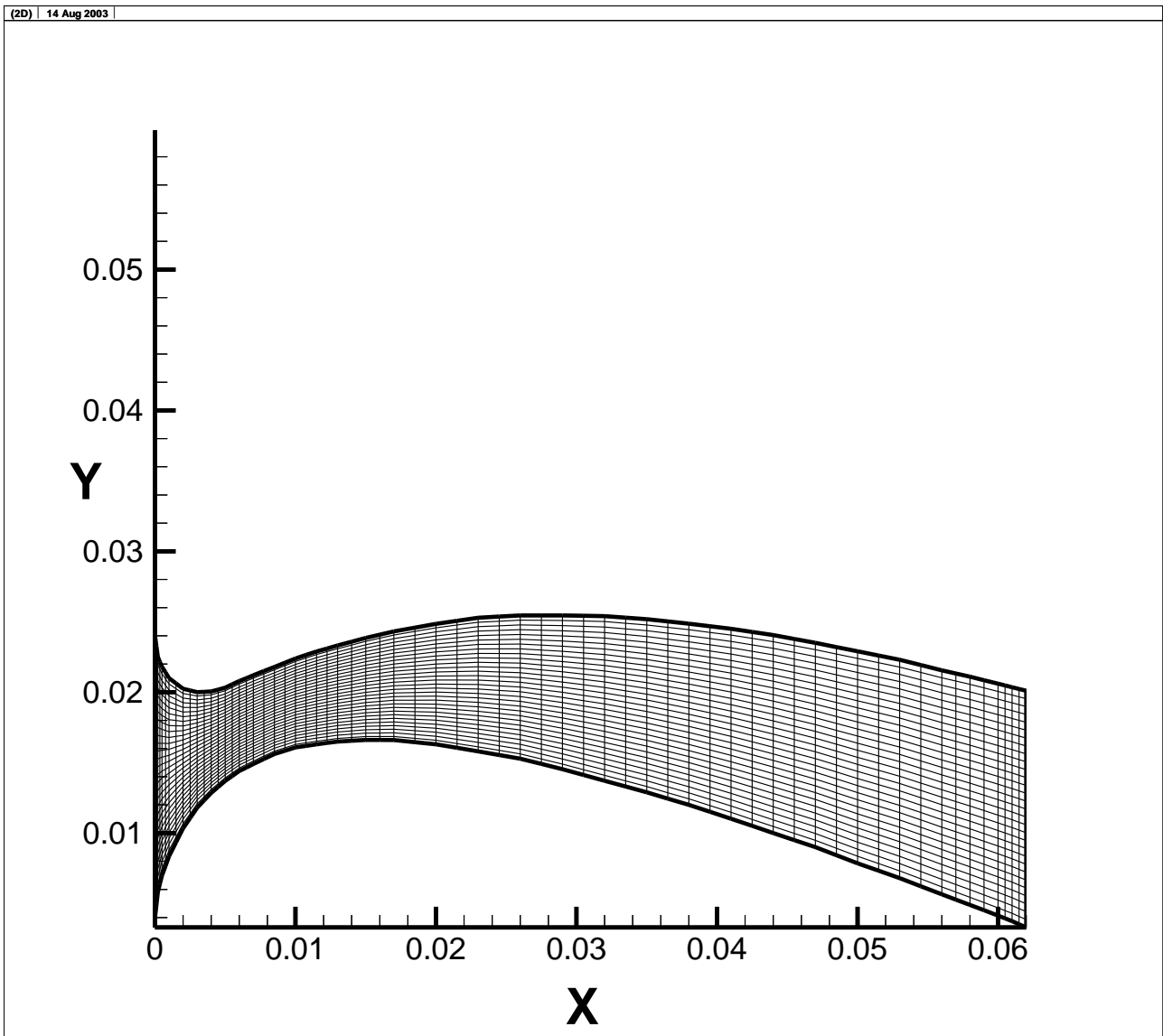


Fig (۳.۳) Physical Domain

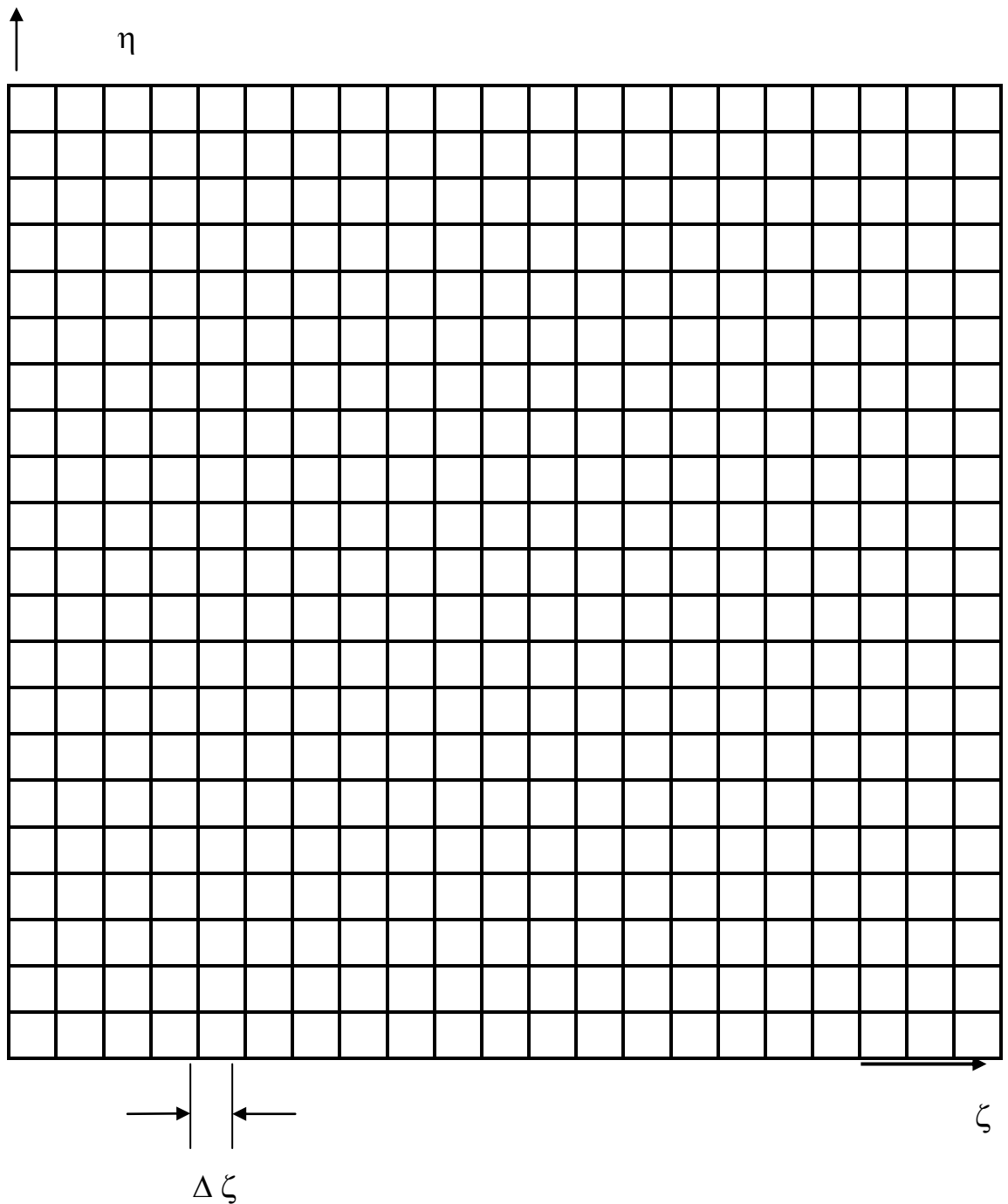


Fig (۳.۴) The rectangular computational domain with uniform grid spacing

equations (۳a) and (۳b) are expressed in a matrix form as:

$$\begin{bmatrix} dx \\ dy \end{bmatrix} = \begin{bmatrix} x_{\xi} & x_{\eta} \\ y_{\xi} & y_{\eta} \end{bmatrix} \begin{bmatrix} d\xi \\ d\eta \end{bmatrix} \quad \dots\dots\dots (۳)$$

Reversing the role of the independent variables, we may write

$$d\xi = \xi_x dx + \xi_y dy \quad \dots\dots\dots (۴a)$$

$$d\eta = \eta_x dx + \eta_y dy \quad \dots\dots\dots$$

(۴b)

$$\begin{bmatrix} d\xi \\ d\eta \end{bmatrix} = \begin{bmatrix} \xi_x & \xi_y \\ \eta_x & \eta_y \end{bmatrix} \begin{bmatrix} dx \\ dy \end{bmatrix} \quad \dots\dots\dots (۴)$$

Multiplying both sides of equation (۳) by

$$\begin{bmatrix} x_{\xi} & x_{\eta} \\ y_{\xi} & y_{\eta} \end{bmatrix}^{-1}$$

yields

$$\begin{bmatrix} d\xi \\ d\eta \end{bmatrix} = \begin{bmatrix} x_{\xi} & x_{\eta} \\ y_{\xi} & y_{\eta} \end{bmatrix}^{-1} \begin{bmatrix} dx \\ dy \end{bmatrix} \quad \dots\dots\dots$$

(۴)

comparing equation (۴) and (۴) yields

$$\begin{bmatrix} \xi_x & \xi_y \\ \eta_x & \eta_y \end{bmatrix} = \begin{bmatrix} x_{\xi} & x_{\eta} \\ y_{\xi} & y_{\eta} \end{bmatrix}^{-1} \quad \dots\dots\dots$$

(۴)

let

$$A = \begin{bmatrix} \xi_x & \xi_y \\ \eta_x & \eta_y \end{bmatrix}$$

..... (۴۸)

$$(۴۹) \quad \mathbf{A}^{-1} = \begin{bmatrix} x_{\xi} & x_{\eta} \\ y_{\xi} & y_{\eta} \end{bmatrix} \quad \dots\dots\dots$$

Using Gramers rule. We can solve equation (۴۶) for the two unknowns

$\frac{\partial}{\partial x}$ and $\frac{\partial}{\partial y}$ for $\frac{\partial}{\partial \xi}$ as follows:

$$\frac{\partial}{\partial \xi} = \frac{\begin{vmatrix} \frac{\partial}{\partial x} & \frac{\partial \eta}{\partial x} \\ \frac{\partial}{\partial y} & \frac{\partial \eta}{\partial y} \end{vmatrix}}{\begin{vmatrix} \frac{\partial \xi}{\partial x} & \frac{\partial \eta}{\partial x} \\ \frac{\partial \xi}{\partial y} & \frac{\partial \eta}{\partial y} \end{vmatrix}} \quad \dots\dots\dots$$

The determinate in the denominator of equation (۵۰) is the Jacobian of transformation (J) defined by:

$$\mathbf{J} = \frac{\partial(\xi, \eta)}{\partial(x, y)} = \begin{vmatrix} \xi_x & \eta_x \\ \xi_y & \eta_y \end{vmatrix} \quad \dots\dots\dots$$

$$\mathbf{J} = \frac{1}{\mathbf{J}^{-1}} = \frac{1}{\frac{\partial(x, y)}{\partial(\xi, \eta)}} = \frac{1}{\begin{vmatrix} x_{\xi} & x_{\eta} \\ y_{\xi} & y_{\eta} \end{vmatrix}} \quad \dots\dots\dots$$

$$\frac{\partial}{\partial \xi} = \frac{1}{\mathbf{J}} \left[\eta_y \frac{\partial}{\partial x} - \eta_x \frac{\partial}{\partial y} \right] \quad \dots\dots\dots$$

from equation (29) and (30) it follows:

$$J = \frac{1}{\begin{vmatrix} A^{-1} \end{vmatrix}} = \frac{1}{\begin{vmatrix} x_\xi & y_\eta \\ -y_\xi & x_\eta \end{vmatrix}} \dots\dots\dots$$

$$A = \begin{vmatrix} A^{-1} \end{vmatrix}^{-1} = \frac{\text{Transpose of cofactor } A^{-1}}{\begin{vmatrix} A^{-1} \end{vmatrix}} \dots\dots\dots$$

Transpose of cofactor

$$A^{-1} = \begin{bmatrix} y_\eta & -x_\eta \\ -y_\xi & x_\xi \end{bmatrix}$$

.....(36)

Substituting equations (28), (35), and (36) in equation (30) yields

$$A = J \begin{bmatrix} y_\eta & -x_\eta \\ -y_\xi & x_\xi \end{bmatrix} \dots\dots\dots (37)$$

The elements of matrix **A** may be obtained by:

$$\xi_x = J y_\eta \dots\dots\dots (38a)$$

$$\eta_x = -J y_\xi \dots\dots\dots$$

$$\eta_y = J x_\xi \dots\dots\dots$$

(38c)

(38d)

Where \mathbf{J} is defined by equation (9.8)

To compute the matrices numerically, equations (9.8) are used, the matrices (x_ξ, x_η, \dots) are computed initially, from which the Jacobian may be evaluated. These expressions are computed numerically by using finite difference approximations; in this case a second-order central difference approximation may be used to compute the transformation derivative for the interior grid points [9].

$$x_\xi = \frac{x_{i+1,j} - x_{i-1,j}}{2\Delta\xi} \dots\dots\dots(9a)$$

$$x_\eta = \frac{x_{i,j+1} - x_{i,j-1}}{2\Delta\eta} \dots\dots\dots(9b)$$

$$y_\xi = \frac{y_{i+1,j} - y_{i-1,j}}{2\Delta\xi} \dots\dots\dots(9c)$$

$$(9d) \quad y_\eta = \frac{y_{i,j+1} - y_{i,j-1}}{2\Delta\eta} \dots\dots\dots$$

The transformation derivatives at the boundaries are evaluated with forward or backward second-order approximations, for example, x_η at the $j=1$ boundary is computed by using the forward difference approximation

$$x_\eta = \frac{-3x_{i,1} + 4x_{i,2} - x_{i,3}}{2\Delta\eta} \dots\dots\dots(9e)$$

The desired number of grid points defined by

IM (the maximum number of grid points in ξ) and JM (the maximum number of grid points in η) is specified. The equal grid spacing in the computational domain is produced as follows:

$$\Delta \xi = \frac{1}{IM-1} \dots\dots\dots (71a)$$

$$\Delta \eta = \frac{1}{JM-1} \dots\dots\dots (71b)$$

The interpretation of the metrics is obvious considering the following approximation:

$$\xi_x = \frac{\partial \xi}{\partial x} \cong \frac{\Delta \xi}{\Delta x} \dots\dots\dots (72)$$

This expression indicates that the metrics represent the ratio of lengths in the computational space to that in the physical space.

۳.۳ Analytical solution

۳.۳.۱ Introduction

Time-dependent solutions of the Euler equations are now widely used for the analysis of the flow through turbomachine blade rows. Their main attraction is the ability to compute mixed subsonic-supersonic flows with automatic capturing of shock waves. Solutions of the potential flow equation have also recently been

extended to compute transonic shocked flow

.Although these can be computationally much more efficient than solutions of the Euler equations, the limitation to potential flow rules them out for applications where strong shock waves can occur. Solving the Euler equations is also the most common way of computing fully three-dimensional flow in turbomachinery, even for subsonic flow.

The equations may be solved in either a finite difference or a finite volume form. In the former (e.g., Veuillot, Gliebe) it is usual to transform the computational domain into a uniform rectangular grid and to express the derivatives of the flow variables in terms of values at the nodes at this grid. Specialized numerical technique such as MacCormack schemes is needed to ensure stability of the integration [9].

3.3.2 Equations for Inviscid Flow (Euler Equations)

Inviscid flow is, by definition flow where the dissipative, transport phenomena of viscosity, mass diffusion, and thermal conductivity are neglected. Therefore the resulting equations for unsteady, inviscid, non-heat conduction, compressible, two dimensional flow called (Euler Equations) expressed in a conservation form are [10]:

Continuity equation

$$\frac{\partial \rho}{\partial t} + \frac{\partial(\rho u)}{\partial x} + \frac{\partial(\rho v)}{\partial y} = 0 \quad \dots\dots\dots$$

Momentum equations

X component:

$$\frac{\partial(\rho u)}{\partial t} + \frac{\partial(\rho u^2 + p)}{\partial x} + \frac{\partial(\rho uv)}{\partial y} = 0 \quad \dots\dots\dots$$

Y component:

$$\frac{\partial(\rho v)}{\partial t} + \frac{\partial(\rho uv)}{\partial x} + \frac{\partial(\rho v^2 + p)}{\partial y} = 0 \quad \dots\dots\dots$$

(10)

The conservation of energy equation is

$$\frac{\partial(\rho e_o)}{\partial t} + \frac{\partial(\rho e_o u + pu)}{\partial x} + \frac{\partial(\rho e_o v + pv)}{\partial y} = 0 \quad \dots\dots\dots$$

(११)

३.३.३ Vector Form of Euler Equations

The first perspective is simply that the conservation form of the governing equations provides a numerical and computer-programming convenience in that the continuity, momentum, and energy equations in conservation form can all be expressed by the same generic equation. Therefore, the compressible Euler equations in Cartesian coordinates without body forces or external heat addition can be written in vector form as [१०]:

$$\frac{\partial Q}{\partial t} + \frac{\partial E}{\partial x} + \frac{\partial F}{\partial y} = 0 \quad \dots\dots\dots (११)$$

Where:

Q, E, and F are vectors given by: -

$$Q = \begin{bmatrix} \rho \\ \rho u \\ \rho v \\ \rho e_o \end{bmatrix} \quad \dots\dots\dots (१२)$$

$$E = \begin{bmatrix} \rho u \\ \rho u^2 + p \\ \rho uv \\ \rho e_o u + pu \end{bmatrix} \quad \dots\dots\dots (१३)$$

$$F = \begin{bmatrix} \rho v \\ \rho uv \\ \rho v^2 + p \\ \rho e_o v + pv \end{bmatrix} \quad \dots\dots\dots (१४)$$

For the problem of interest where only steady flow solutions are required the energy equation may be replaced with the assumption that the stagnation enthalpy is constant every where. The energy equation is eliminated in favor of the steady adiabatic flow relation.

3.3.4 **Body-Fitted Coordinate System**

System

The need to satisfy the boundary conditions exactly led to the development of body-fitted coordinates. Such coordinates are difficult to generate for complex bodies. Even when they are generated, one has to contend with singularities that require special treatment [^]. In body-fitted coordinate system , flow boundary surface such as blade profile shapes become coordinate lines in the computational space. The advantage of such systems is evident when incorporating boundary conditions in a finite difference computation.

3.3.5 Euler Equations in Body-Fitted coordinates

Sets of surface-oriented curvilinear coordinates, denoted by $\xi(x, y), \eta(x, y)$ are introduced in order to facilitate treatment of arbitrary flow regions. Therefore ,the Euler equations can be transformed from Cartesian coordinates to general curvilinear coordinates.

The Euler Equation in curvilinear coordinates in vector form can be given by [20, 28]:

$$\frac{\partial \bar{Q}}{\partial t} + \frac{\partial \bar{E}}{\partial \xi} + \frac{\partial \bar{F}}{\partial \eta} = 0 \dots\dots\dots (V1)$$

Where \bar{Q}, \bar{E} and \bar{F} are vectors given by: -

$$\bar{Q} = \frac{1}{J} \begin{bmatrix} \rho \\ \rho u \\ \rho v \end{bmatrix} \dots\dots\dots (V2)$$

$$\bar{E} = \frac{1}{J} \begin{bmatrix} \rho U \\ \rho u U + \xi_x p \\ \rho v U + \xi_y p \end{bmatrix} \dots\dots\dots (V3)$$

$$\bar{F} = \frac{1}{J} \begin{bmatrix} \rho V \\ \rho u V + \eta_x p \\ \rho v V + \eta_y p \end{bmatrix} \dots\dots\dots (V4)$$

Where the contravariant velocity components U and V are defined by:

$$U = \xi_x u + \xi_y v \quad \dots\dots\dots (75)$$

$$V = \eta_x u + \eta_y v \quad \dots\dots\dots (76)$$

The Jacobian transformation J is defined in: -

$$J = \frac{1}{x_\xi y_\eta - x_\eta y_\xi} \quad \dots\dots\dots (77)$$

3.3.6 Explicit Time-Marching Method

Explicit time marching procedures are generally used to solve the Euler equations. However, the computational time required by that procedure to arrive at an accurate solution is often prohibitive. In explicit schemes, the spatial derivatives are evaluated using known conditions at the old time level. The explicit schemes are used widely for the computation of turbo machinery flows and solving nonlinear PDE's [1].

The predictor-corrector method proposed by MacCormack [1969] is widely used for both internal and external flows. The method is second-order-accurate in both time and space. It can be used for both steady and unsteady compressible flows as well as for viscous and inviscid flows.

In the MacCormack method a two-step predictor-corrector sequence is used with forward difference on the predictor and backward difference on the corrector, is a second-order-accurate method.

By means of a Taylor series expansion, the flow-field variables are advanced at each grid point (i, j) in steps of time, as shown below [24, 29]:

$$\bar{Q}_{i,j}^{n+1} = \bar{Q}_{i,j}^n + \left(\frac{\partial \bar{Q}}{\partial t} \right)_{av} \Delta t \quad \dots\dots\dots (78)$$

Where, once again \bar{Q} is a flow-field variable

(from the governing equations) assumed known at time n, either from initial conditions or as a result from the previous iteration in time, $\left(\frac{\partial \bar{Q}}{\partial t}\right)_{av}$ is defined as

$$\left(\frac{\partial \bar{Q}}{\partial t}\right)_{av} = \frac{1}{2} \left[\left(\frac{\partial \bar{Q}}{\partial t}\right)_{i,j}^n + \left(\frac{\partial \bar{Q}}{\partial t}\right)_{i,j}^{n+1} \right] \dots\dots\dots (V9)$$

To obtain a value of $\left(\frac{\partial \bar{Q}}{\partial t}\right)_{av}$, the following steps are taken:

1. $\left(\frac{\partial \bar{Q}}{\partial t}\right)_{i,j}^n$ is calculated using forward spatial differences on the right-hand side of the governing equations from the known flow field at time n.

2. From step 1 PREDICTED values of the flow –field variables can be obtained at time n+1 as follows:
 $\bar{Q}_{i,j}^{n+1'} = \bar{Q}_{i,j}^n + \left(\frac{\partial \bar{Q}}{\partial t}\right)_{i,j}^n \Delta t$

Combining steps 1 and 2, predicted values are determined as follows:

$$\bar{Q}_{i,j}^{n+1'} = \bar{Q}_{i,j}^n - \frac{\Delta t}{\Delta \xi} \left[\bar{E}_{i+1,j}^n - \bar{E}_{i,j}^n \right] - \frac{\Delta t}{\Delta \eta} \left[\bar{F}_{i,j+1}^n - \bar{F}_{i,j}^n \right] \dots\dots\dots (A1)$$

3. Using backward spatial differences, the predicted values (from step 2) are inserted into the governing equations such that a predicted time derivative $\left(\frac{\partial \bar{Q}}{\partial t}\right)_{i,j}^{n+1'}$ can be obtained.

$$\bar{Q}_{i,j}^{n+1'} = \bar{Q}_{i,j}^n - \frac{\Delta t}{\Delta \xi} \left[\bar{E}_{i,j}^{n+1'} - \bar{E}_{i-1,j}^{n+1'} \right] - \frac{\Delta t}{\Delta \eta} \left[\bar{F}_{i,j}^{n+1'} - \bar{F}_{i,j-1}^{n+1'} \right] \dots\dots\dots (A2)$$

ξ. Finally, substitute $\left(\frac{\partial \bar{Q}}{\partial t}\right)_{i,j}^{n+1'}$ from step 3 into

equation (19) to obtain CORRECTED second-order-accurate values \bar{Q} at time

$n+1$. As in equation (1) steps 3 and ξ are combined as follows:

$$\bar{Q}_{i,j}^{n+1} = \frac{1}{2} \left[\bar{Q}_{i,j}^n + \bar{Q}_{i,j}^{n+1'} - \frac{\Delta t}{\Delta \xi} \left(\bar{E}_{i,j}^{n+1'} - \bar{E}_{i-1,j}^{n+1'} \right) - \frac{\Delta t}{\Delta \eta} \left(\bar{F}_{i,j}^{n+1'} - \bar{F}_{i,j-1}^{n+1'} \right) \right] \dots \dots \dots \quad (13)$$

Steps 1 to ξ are repeated until the flow-field variables approach a steady-state value this is the desired steady-state solution.

3.3.4 Artificial Viscosity

MacCormack and Baldwin (1970) added an artificial viscosity or dissipation term in the Navier-Stokes equation. This provides the necessary stability to the code [1]. The Euler equations omit viscosity; however, discretization generally reintroduces viscosity or, more precisely, second-difference terms that have viscous-like effects. Second differences that arise naturally as a part of first-derivative approximation are called implicit artificial viscosity. Second differences purposely added to first-derivative approximations are called explicit artificial viscosity. Artificial viscosity forms sometimes suggest alterations and improvements. The implicit artificial viscosity is too small, making unstable, and adding explicit second-order artificial viscosity with a positive coefficient has a smoothing and stabilizing effect. In other cases, a numerical method may have too much artificial viscosity, causing smearing or even instability. In this case adding explicit artificial viscosity with a negative coefficient partially cancels the implicit artificial viscosity, resulting in a sharper, and even more stable solution. Second-order artificial viscosity with a positive coefficient is sometimes called artificial dissipation; second-order artificial viscosity with a negative coefficient is sometimes also called artificial antidissipation [19, 30].

The fourth order smoothing term

amounts to adding to the predictor and corrector steps the difference form of the following term:

Predictor step

$$\left(\bar{Q}^{n+1'}\right)_{i,j} = \left(\bar{Q}_{1s}^{n+1'}\right)_{i,j} + \left(S\bar{Q}^{n+1'}\right)_{i,j} \dots\dots\dots (14)$$

Where

$$\left(\bar{Q}_{1s}^{n+1'}\right)_{i,j} = \bar{Q}_{i,j}^n - \frac{\Delta t}{\Delta \xi} \left[\left(\bar{E}_1^n\right)_{i+1,j} - \left(\bar{E}_1^n\right)_{i,j} \right] - \frac{\Delta t}{\Delta \eta} \left[\left(\bar{F}_1^n\right)_{i,j+1} - \left(\bar{F}_1^n\right)_{i,j} \right] \dots\dots\dots (15)$$

And $(S\bar{Q}_1^{n+1'})_{i,j}$ is a fourth order artificial viscosity term, defined by [19]

$$\begin{aligned} \left(S\bar{Q}_1^{n+1'}\right)_{i,j} &= \frac{C_\xi \left| P_{i+1,j}^n - 2P_{i,j}^n + P_{i-1,j}^n \right|}{\left(P_{i+1,j}^n + 2P_{i,j}^n + P_{i-1,j}^n \right)} \left[\left(\bar{Q}_1^n\right)_{i+1,j} - 2\left(\bar{Q}_1^n\right)_{i,j} + \left(\bar{Q}_1^n\right)_{i-1,j} \right] \\ &+ \frac{C_\eta \left| P_{i,j+1}^n - 2P_{i,j}^n + P_{i,j-1}^n \right|}{\left(P_{i,j+1}^n + 2P_{i,j}^n + P_{i,j-1}^n \right)} \left[\left(\bar{Q}_1^n\right)_{i,j+1} - 2\left(\bar{Q}_1^n\right)_{i,j} + \left(\bar{Q}_1^n\right)_{i,j-1} \right] \dots\dots\dots (16) \end{aligned}$$

Corrector step

$$\left(\bar{Q}^{n+1}\right)_{i,j} = \left(\bar{Q}_{1s}^{n+1}\right)_{i,j} + \left(S\bar{Q}^{n+1}\right)_{i,j} \dots\dots\dots$$

Where

$$\left(\bar{Q}_{1s}^{n+1}\right)_{i,j} = \frac{1}{2} \left[\begin{aligned} &\left(\bar{Q}_1^n\right)_{i,j} + \left(\bar{Q}_1^{n+1'}\right)_{i,j} - \frac{\Delta t}{\Delta \xi} \left[\left(\bar{E}_1^{n+1'}\right)_{i,j} - \left(\bar{E}_1^{n+1'}\right)_{i-1,j} \right] \\ &- \frac{\Delta t}{\Delta \eta} \left[\left(\bar{F}_1^{n+1'}\right)_{i,j} - \left(\bar{F}_1^{n+1'}\right)_{i,j-1} \right] \end{aligned} \right] \dots\dots\dots (17)$$

And

$$\left(\overline{SQ}_1^{n+1} \right)_{i,j} = \frac{C_\xi \left(P_{i+1,j}^{n+1'} - 2P_{i,j}^{n+1'} + P_{i-1,j}^{n+1'} \right)}{\left(P_{i+1,j}^{n+1'} + 2P_{i,j}^{n+1'} + P_{i-1,j}^{n+1'} \right)} \left[\left(\overline{Q}_1^{n+1'} \right)_{i+1,j} - 2 \left(\overline{Q}_1^{n+1'} \right)_{i,j} + \left(\overline{Q}_1^{n+1'} \right)_{i-1,j} \right]$$

$$+ \frac{C_\eta \left(P_{i,j+1}^{n+1'} - 2P_{i,j}^{n+1'} + P_{i,j-1}^{n+1'} \right)}{\left(P_{i,j+1}^{n+1'} + 2P_{i,j}^{n+1'} + P_{i,j-1}^{n+1'} \right)} \left[\left(\overline{Q}_1^{n+1'} \right)_{i,j+1} - 2 \left(\overline{Q}_1^{n+1'} \right)_{i,j} + \left(\overline{Q}_1^{n+1'} \right)_{i,j-1} \right] \dots\dots\dots (\text{A}9)$$

The fourth order nature can be seen in the numerators, which are products of two second-order central difference expressions for second derivatives. C_ξ and C_η are arbitrary specified parameters, with typical values range from 0.1 to 0.3 [29].

The convergence means that the solution to the finite-difference equation approaches the true solution to the partial differential equation having the same initial and boundary conditions as the mesh refined. The time step must be calculated from the Courant-Fridrich-Lewy (CFL) stability criteria, it must be less than, or at best equal to the time taken by a sound wave to travel from one grid point to the next. The solution becomes unstable when CFL is greater than one.

Convergence criterion to reach steady state solution is based on the maximum change in pressure between two successive time integrated steps for each grid point, which should be less or equal to 10^{-5}

$$\frac{p^{n+1} - p^n}{p^n} \leq 10^{-5}$$

..... (90)

3.3.8 Calculation Steps

The main steps of explicit two-dimension solution of McCormack's technique may be summarized as follow:

1. Generating grid points in the physical domain.
2. Initializing the value of p , u , v , T and ρ for all grid points in the computational domain.
3. Computing the surfaces bounding the physical domain and generate the grid for computational domain (in ξ and η coordinates).
4. Evaluating the Jacobian transformation parameters for each grid point.
5. Evaluate the values of flux vector \bar{Q} , \bar{E} and \bar{F} for all grid points at time level n .
6. Initializing the value of time step at predictor step.
7. Applying finite difference equations at predictor step and compute $\bar{Q}_1^{n+1'}$, $\bar{Q}_2^{n+1'}$ and $\bar{Q}_3^{n+1'}$ for all grids points.
8. Computing ρ , u , v , T and p using equation (90).
9. Evaluating $\bar{E}_1^{n+1'}$, $\bar{E}_2^{n+1'}$, $\bar{E}_3^{n+1'}$, $\bar{F}_1^{n+1'}$, $\bar{F}_2^{n+1'}$ and $\bar{F}_3^{n+1'}$ at predictor step.
10. Repeating steps (7-9) for corrector step.
11. Computing flow parameters ρ , u , v , T and p at all grid points.
12. Checking the convergence of solution equation (90), if not satisfied advance one time step and repeat steps (7-11).

٣.٤ THE COMPUTER PROGRAMS

٣.٤.١ Introduction

An iterative Quick Basic program was written for the preliminary design of the axial flow gas turbine blade.

Fig (٣.٥) shows the flow chart of aerodynamic design of gas turbine.

٣.٤.٢ Input Data

The input data required to run the program is as follows:

Specific heat ratio

Specific heat at constant pressure

Inlet stagnation pressure

Inlet stagnation temperature Rotational speed

Inlet Mach number

٣.٤.٣ Program output

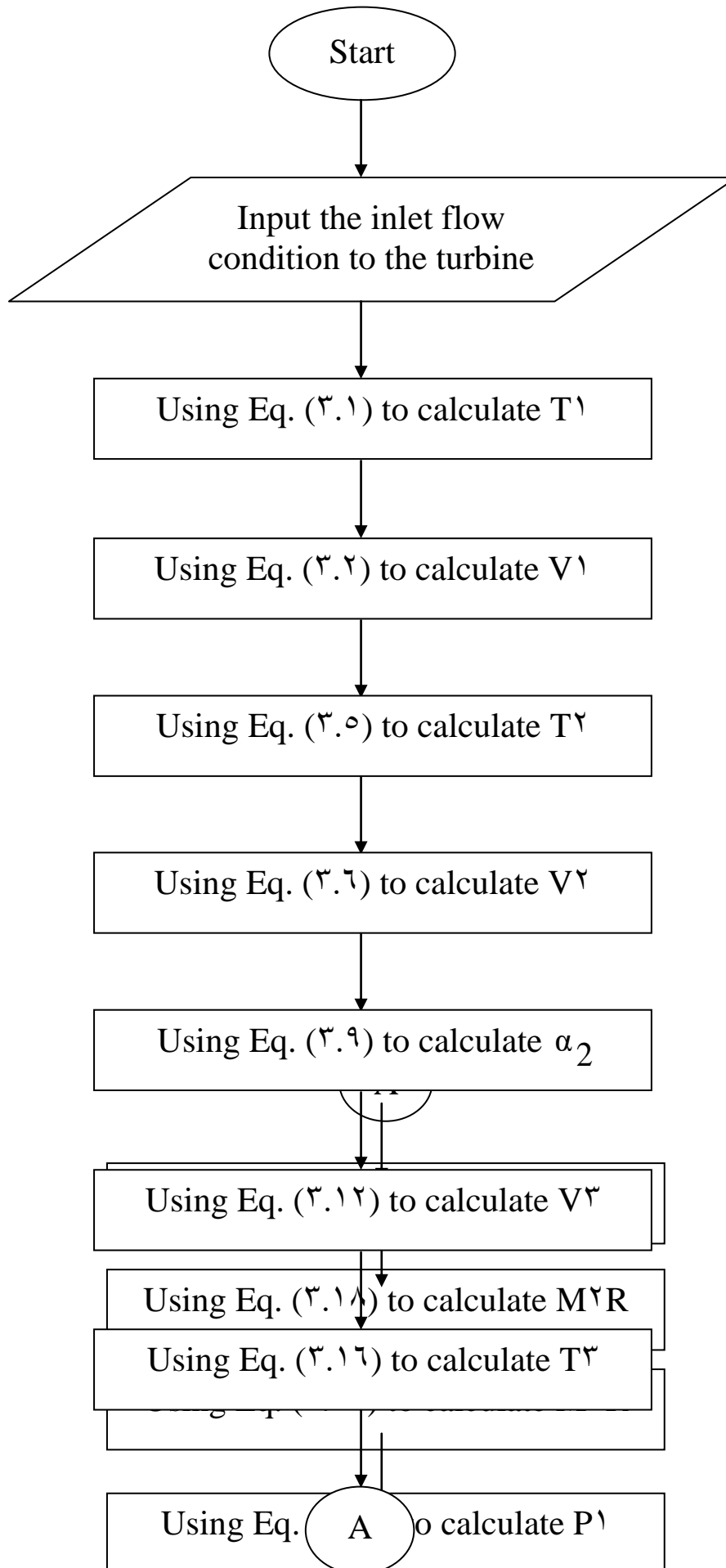
The outputs from the program are as follows:

The static properties (P,T,ρ)

The total properties (T_t , P_t)

Thermal efficiency (η_t)

Fig (3.6) shows the flow chart for two dimensions explicit method.



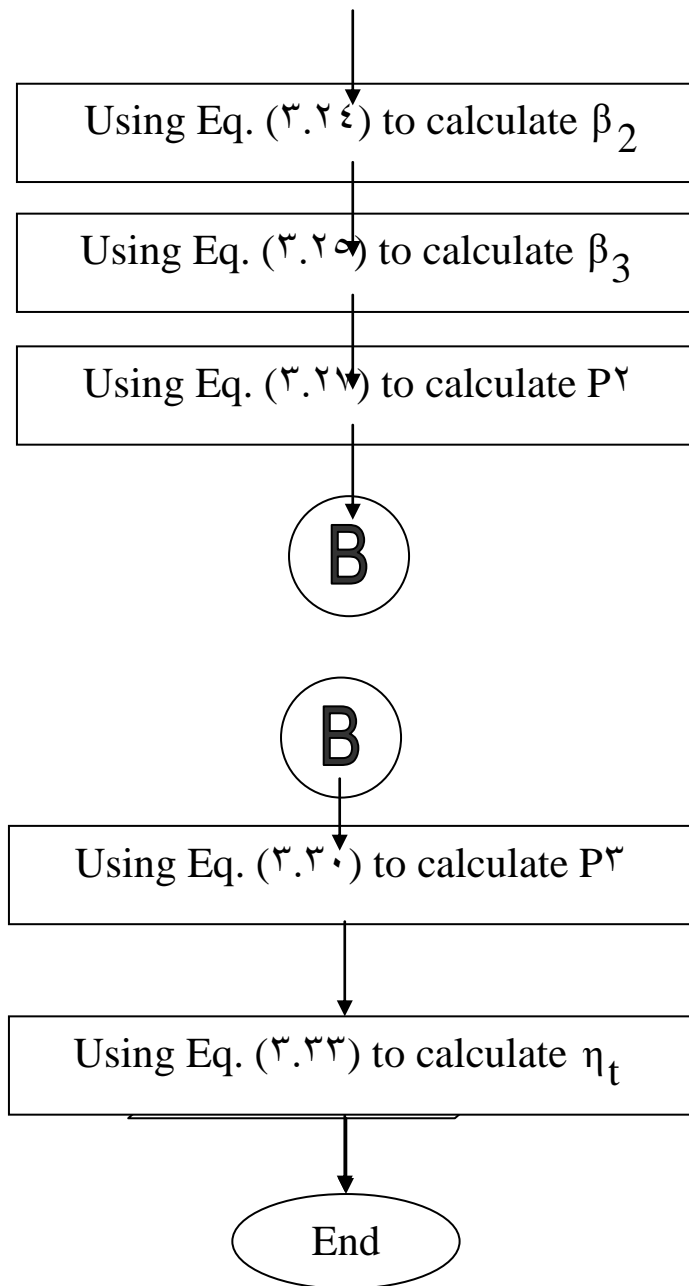
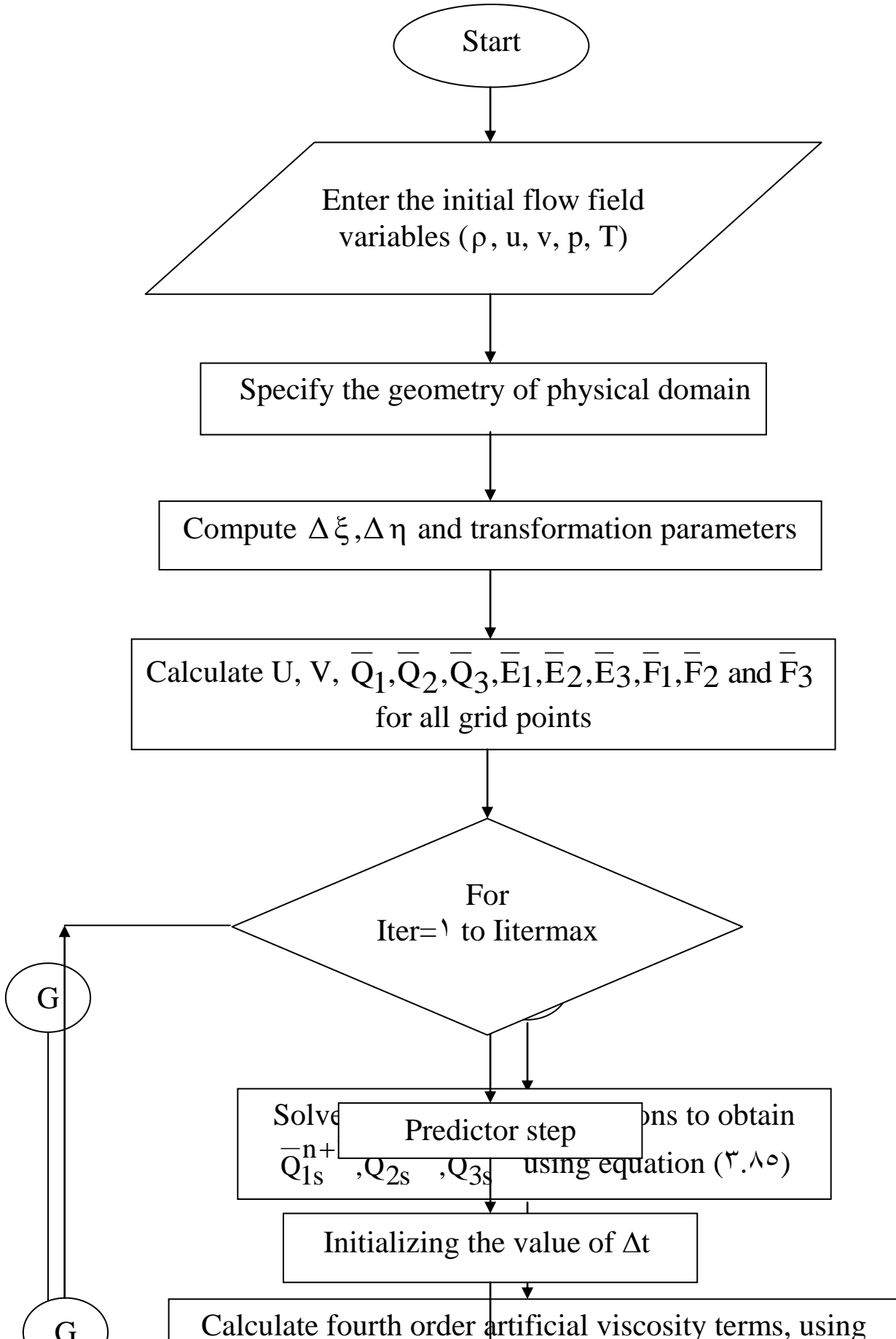
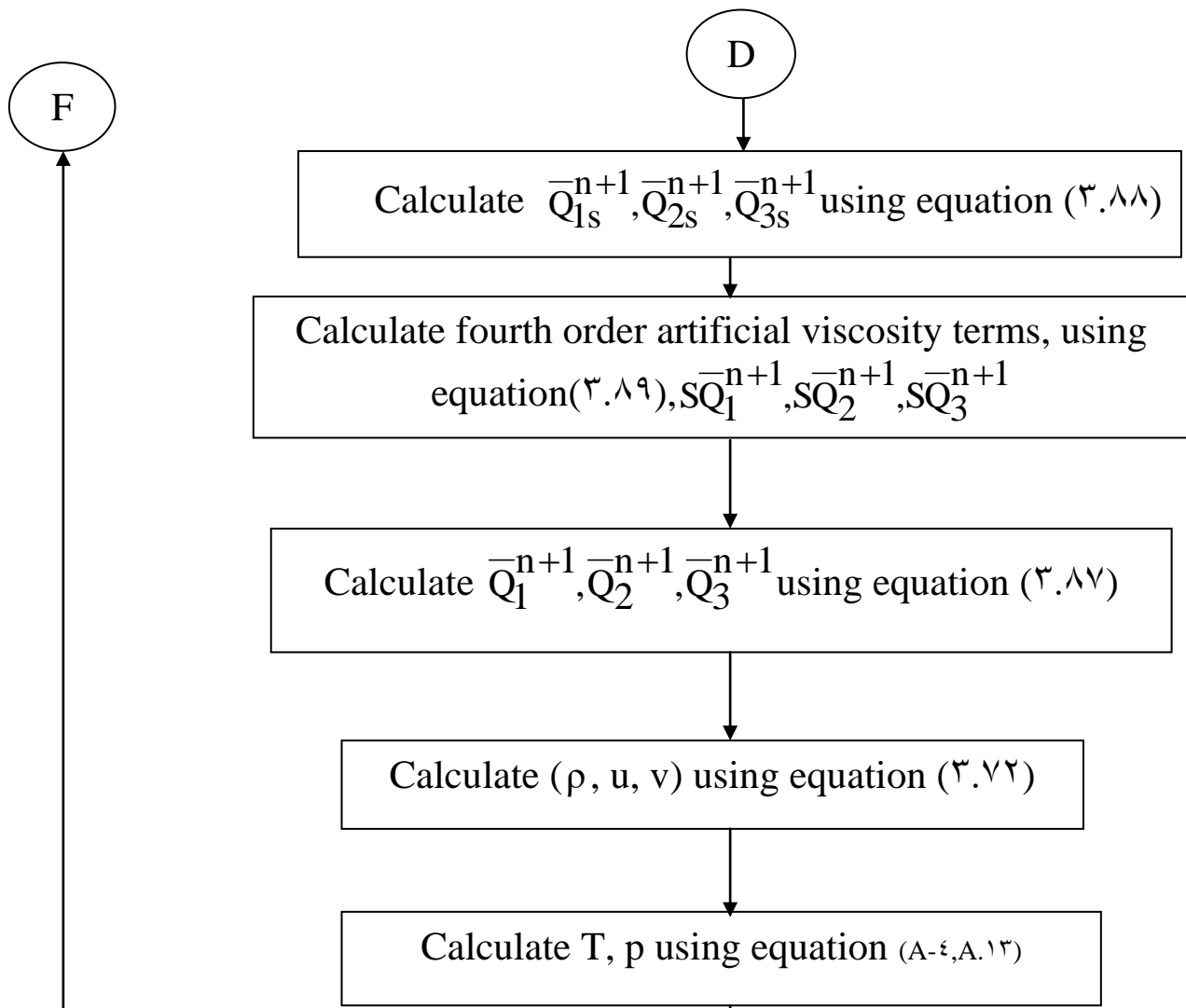


Fig (3.9)

Flow chart of the aerodynamic design of gas turbine





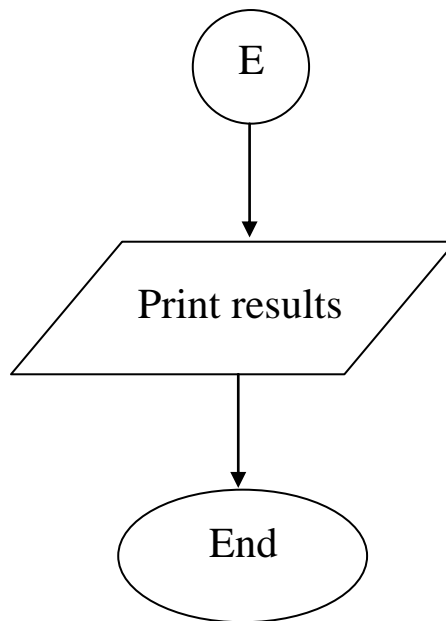
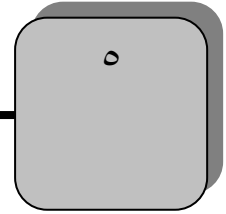


Fig (٣.٦)
The flow chart for two dimensions explicit method

Chapter Five

Conclusion and Recommendations



۵.۱ Conclusion

The following points can be concluded :-

۱. In the stator blade, the fluid is accelerated while the static pressure decreases and the tangential velocity of fluid is increased in the direction of rotation.

۲. The rotor decreases the tangential velocity in the direction of rotation; tangential forces are exerted by the fluid on the rotor blades, and the fluid velocity is reduced across the rotor.

۳. The large turning in rotor is possible reaching up to ۱۴۰ deg. because, usually, the flow is accelerating through blade row. This means that the static pressure drops across the rotor.

۴. The efficiency of rotor blade depends upon the blade speed ratio and inlet absolute flow angle to the rotor, therefore the maximum value of blade speed should be considered in the design conditions to the limitations of the rotational speed.

۵. The value of rotational speed should be limited according to the mean diameter of turbine rotor to improve blade efficiency.

۶. The addition of artificial viscosity has eliminated the oscillations that were encountered in the case with no artificial viscosity.

۷. When analyzing the flow through the blades of axial flow gas turbine, there is no difference between the results at the number of

iteration 2000 and 3000, because the solution reaches at the convergence at the number of iteration 2000.

^In case I the number required of rotor blades is 27 and the required number of stator blades is 28. In case II the number required of rotor blades is 22 and the required stator number of blades is 26.

5.2 Recommendations for future work:

The following recommendation may be stated for the future work:

1. Use three-dimensional analysis for solving Euler equations.
2. Study a viscous flow analysis and studying the difference in flow calculation results between the inviscid and viscous flow analysis.
3. Study the stresses and forces on the rotor blade by using the flow calculation results.

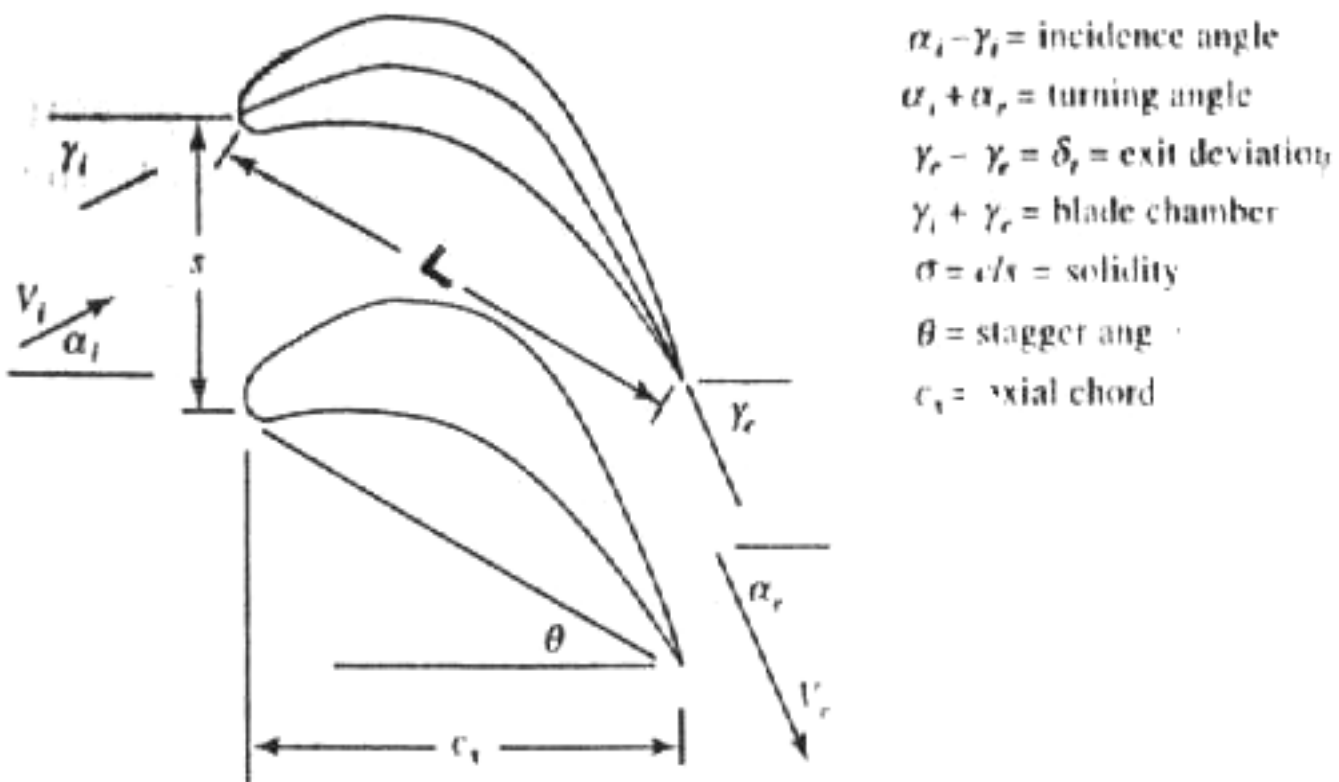


Fig (۳.۲) Blade angles

REFERENCES

- [၁] Budugur Lakshminarayana,"Fluid Dynamics and Heat transfer turbomachinery", John Willey and Sons, Inc., ၁၉၉၆.
- [၂] Horlock, J.H,"Axial Flow Turbines" Robert E.Krieger Puplising company, New York, ၁၉၇၃.
- [၃] Cohen H., Rogers G.F.C. and H.I.H.Saravanamnttoo,"Gas Turbine Theory", John Wiley and Sons, Inc., New York, ၁၉၈၇.
- [၄] Pratt and Whitney,"A multiple-Grid Scheme for Solving the Euler Equations", AIAA Journal, Vol.၂၀, No.၁၁, November ၁၉၈၂.
- [၅].Denton J.D.,"An Improved Time-Marching Method for Turbomachinery Flow Calculation", Journal of Engineering for Power, Vol.၁၀၀, July ၁၉၈၃.
- [၆] Shmuel Eidelman and Raymond P.Shreeve,"Application of the Godunov Method and Its Second-Order Extension to cascade Flow Modeling", AIAA Journal, Vol.၂၂, No.၁၁, November ၁၉၈၄.
- [၇] Mao S.K.,"A Streamline Curvature Method For calculating S^၁ Stream Surface Flow", Journal of Engineering for Gas Turbines and Power, ASME, Vol.၁၀၆, April ၁၉၈၄.
- [၈] Clarke D. Keith,"Euler Calculations for Multielement Airfoils Using Cartesian Grids", AIAA Journal, Vol.၂၄, No.၃, March ၁၉၈၆.
- [၉] Antony Jameson,"Multigrid Solution of the Euler Equations Using Implicit Schemes", AIAA Journal, Vol.၂၄, No.၁၁, November ၁၉၈၆.
- [၁၀] Young June Moon,"Grid Size Dependence on Convergence for Computation of he Navier-Stokes Equations", AIAA Journal, Vol.၂၄, No.၁၀, October ၁၉၈၆.

[۱۱] Stephen F.Wornom and Mahamed M.Hafez,"Implicit conservative Schemes for the Euler Equations", AIAA Journal, Vol.۲۴, No.۲, February ۱۹۸۶.

[۱۲] Thomas H.Pulliam,"Artificial Dissipation Models for the Euler Equations " AIAA Journal, Vol.۲۴, No.۱۲, December ۱۹۸۶.

[۱۳] Dave M.Belk,"Three-Dimensional Unsteady Euler Equations Solution on Dynamic Grids",AIAA Journal ,Vol.۲۵,No.۹,September ۱۹۸۷.

[۱۴] Von Lavante E.,"Numerical Solutions of Euler Equations Using Simplified Flux Vector Splitting", AIAA Journal, Vol.۲۵, No.۸, August ۱۹۸۷.

[۱۵] Venkatakrishnan V.,"Computation of Unsteady Transonic Flows by the solution of Euler Equations", AIAA Journal, Vol.۲۶, No.۸, August ۱۹۸۸.

[۱۶] Gerolymos G.A.,"Numerical Integration of the Blade-to-blade Surface Euler Equations in Vibrating Cascades", AIAA Journal, Vol.۲۶, No.۱۲, December ۱۹۸۸.

[۱۷] Kwon O.K.,"Navier-Stokes Solution for Steady Two-Dimensional Transonic Cascade Flows", Journal of Turbomachinery, Vol.۱۱۱, July ۱۹۸۸.

[۱۸] Oguz M.S.,"Quasi-Three-Dimensional Numerical Design of Turbomachinery Blades", July ۱۹۹۰.

[۱۹] Matthew D.Montgomery and Joseph M.Verdon,"Athree-Dimensional Linearized Unsteady Euler Analysis For Turbomachinery Blade Rows", June ۱۹۹۶.

- [20] Ning W. and L.He,”Computation of Unsteady Flows Around Oscillating Blades Using Linear and Nonlinear Harmonic Euler Methods”, Journal of Turbomachinery, ASME, Vol. 120, July 1998.
- [21] Demeulenaere A.,”Three-Dimensional Inverse Method for Turbomachinery Blading Design”, Journal of Turbomachinery, Vol. 120, April 1998.
- [22] Amano R.S.,”An Implicit Scheme For Cascade Flow and Heat Transfer Analysis”, Journal of Turbomachinery, Vol. 122, April 2000.
- [23] Mattingly Jack D.,”Elements of Gas Turbine Propulsion”, McGraw-Hill, Inc., 1996.
- [24] Anderson Dale A., John C.Tannehill and Richard H.Pletcher,”Computational Fluid Mechanics and Heat Transfer”, 1984.
- [25] HOFFMANN KLAUS A.,”Computational Fluid Dynamics for engineers”, 1989.
- [26] Joe F.Thompson,”Grid Generation Techniques in Computational Fluid Dynamics”, AIAAJournal, Vol.22, No.11, November 1984.
- [27] Fletcher, C.A.J.,”Computational Techniques for Fluid Dynamics”, Vol.2, Springer-Verlag, 1988.
- [28] Aronone A., Pacciani R.and Sestini A.”Multigrid Computations of Unsteady Rotor-Stator Interaction Using the Navier-Stokes Equations”, Journal of Fluids Engineering, ASME, Vol. 117, December 1995.
- [29] John D.Anderson, Jr.,”Computational Fluid Dynamics”, McGraw-Hill, Inc., 1990.
- [30] Culbert B.Laney,”Computational Gas Dynamics”, 1998.

[۳۱] Sieverding C.H., "The Influence of Trailing Edge Ejection on the Base Pressure in Transonic Turbine Cascades", Journal of Engineering for Power, Vol. ۱۰۵, April ۱۹۸۳.